

# A Statistical Method for Determining the Required Measurement Number of Graphene Sheets Nanoparticles for Quality Control

Afrah Mohammed kadhim

*Middle Technical University, Kut Technical Institute, Kut, Iraq*

*Afrahkadm88@gmail.com*

## Abstract

Commercial products that the graphene usage is fundamental are in their beginning. The traditional graphene manufacturing is recently investigated and their infancy attributes to the lack in standards and robust scales when the comparison and measurements of graphene and carbonic materials are required. In particular the raman spectroscopy is useful in characterization, where multiple spectra are required for quality control and managing. A statistical approach has been proposed and studied for determining the number of different spectra for graphene characterization. The statistical convergence of a large number of Raman measurements have been recorded and described. As well, the graphical approaches were utilized for monitoring the changes in whole statistics and the Monte-Carlo based preface methodology was applied for data analysis to reconfigure computational data for material analysis.

**Keywords:** Graphene, Nanoparticles, Statistics, Quality Control

## Introduction

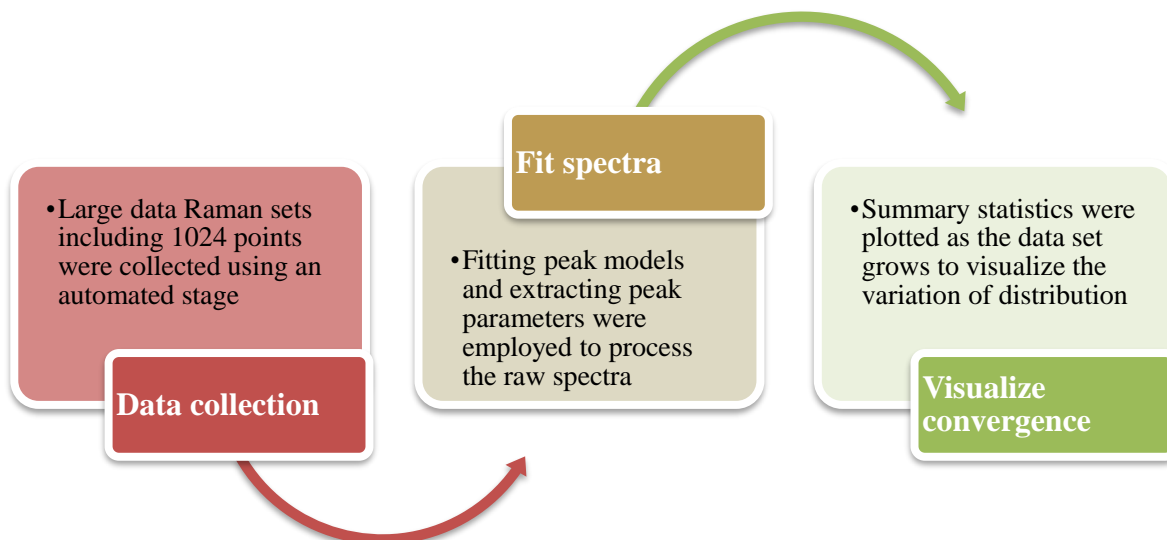
The 1st 2D carbon atomic crystal was graphene [1]. The many unusual characteristics of this substance, like mechanical hardness, intensity, and elasticity in addition to its strong thermal conductivity and electrical conductivity, have given rise to tremendous anticipation since the initial investigation, and graphenes are currently being explored for many various purposes [2]. Secure and sustainable production of carbon materials devices and goods needs careful attention to the potential effect of graphene-enabled substances on public health as well as the environment [3]. However, safety evaluation is an important part of the engineering approaches [4]. The characterization of the Material, in turn, is a key element of hazard assessment. Product characterization, in particular, is a crucial factor in the identification of hazards. The toxicological assessment of nanomaterials is a good example. A decade ago, nanotubes were proposed to show "best-like" antimicrobial activity in experimental animals in the sense that long and stiff, but not small or twisted, carbon nanotubes caused papule development and infection following intravenous infusion in animals [5]. We already realize that carbon nanotubes conform to a so bacterial fiber framework to a certain degree and that this is the case. Some forms of multi-walled graphenes could be regarded as possibly carcinogenic for humans [6]. However, many representatives of a similar class of substances have been shown to become non-toxic [7,8], which can also suffer degradation [9], indicating that perhaps all graphenes are asbestos-like.

In reality, graphene, if properly purified and surface-modified, have exciting potential for nanotechnologies, such as drug delivery and imaging [10]. Numerous graphenes were suggested as possible substances for supercapacitors due to their high electrical properties, high surface area as well as physical flexibility [11]. Reduced graphene oxide, easily developed from graphene oxide, is studied extensively as a template carbon material [12]. Reduced graphene oxide exhibits significant power ability however suffers from a lack of conductance, as reducing carbon materials [13]. Multiple dimensional graphene-based architectures have been studied in order to reduce this recovery by concentrating on adjusting the substance viscosity [14]. Investigating the graphenes filmed structures for ion adsorbents could be another result in adjusting the porosity of the material. Graphitic structure of 3.3 Å interparticle isolation in reconstituted graphene is too limited for ion adsorbents and could be modified with such an intercalant to show an extended film structure [15-18]. It can be hypothesized that certain enlarged filmed structures may have increased ion sorption sites through ion dissolution and confinement impacts as previously shown with CD ultra-micropores [19].

### Methodology of statistical analysis

A selected group of the graphene-related material types were produced and analyzed with the use of 3 separate sets of 1,024 of the Raman spectra that have been obtained from the powder samples for the identification of the guidance for robust collections of the data with statistical significance, all according to work-flow of the Scheme 1. Materials have been selected for covering the wide variety of the topical and interesting carbon nano-materials, especially the graphite, reduced graphene oxide, liquid exfoliated graphene, as well as the high-temperature graphitized carbon. Additionally, 2 of the commercial samples of the graphene nano-platelet (GNP) and the commercial sample of the multi-walled carbon nanotube (MWCNT) have been analyzed. Those samples have been mixed and ground to even fine powder, then pressed in crude pellets for the purpose of ensuring the random flakes' distribution with the minimum spatial dependences; the independent Raman spectra have been gathered afterwards from the points 2.5 $\mu\text{m}$  apart over area that covers 80x80 $\mu\text{m}^2$  for 16h.

All the materials were purchased from Sigma-Aldrich. These measurements have been taken 3 times for each one of the materials (6 for the MWCNT and the graphitized carbon) on another sample every time. The spectra have been assigned, then fitted through the application of the specified procedures. Being in every graphitic carbon material, G band with the Raman shifting of approximately 1580 $\text{cm}^{-1}$  results from de-generate of the in-plane transverse optic and longitudinal optic modes of the phonon, the symmetric opposite carbon atoms movement in one specific direction in the graphene sheets' plane.



**Scheme 1. The statistical analysis guidance of this work.**

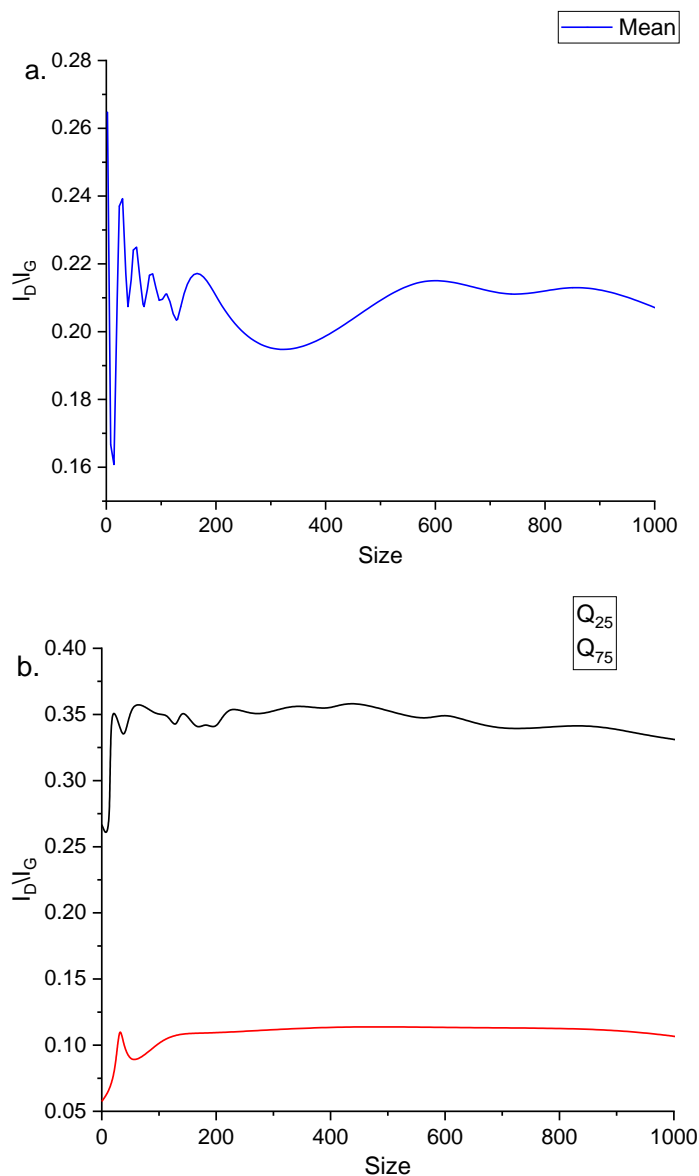
## Results and discussions

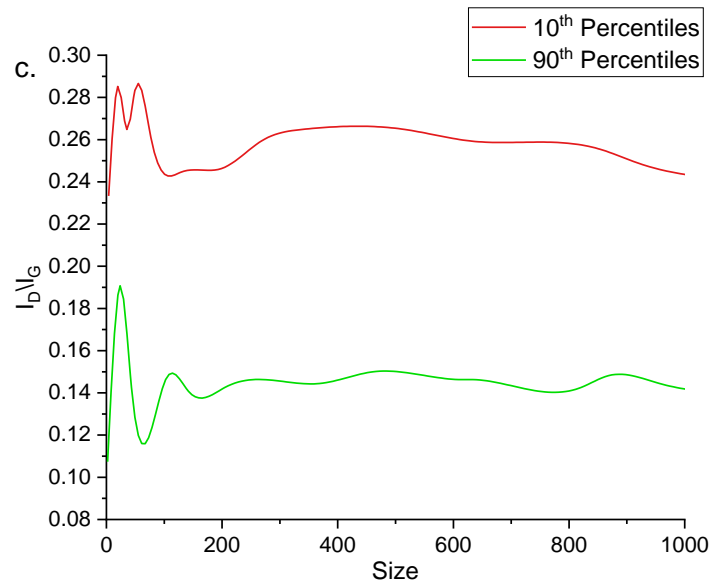
D peak can be described as being more variable in the wave-number and dispersive, however, in general, it appears about  $1,350\text{cm}^{-1}$  and results from the same phonon scattering (iTO mode). None-the-less, such transition needs a 2<sup>nd</sup> event of the scattering from symmetry breaking “flaw” which is bonded to the 6-member ring of the carbon, which is why the “flaw” of the label peaks. The other big peak is 2-D peak which can be seen at higher Raman shift cases around  $2,700\text{cm}^{-1}$  and the often utilized for probing the thickness of the graphene. Energy similarity between photons and transition of excitation makes this process resonant, and as a result, provides it with the sensitivity to the changes in band structure like that observed from the bi-layer and mono-layer graphene, the variable which will alter the peak position, shape, and intensity. Usually,  $I_{2D}/I_G$  and 2-D peak FWHM will be obtained, then utilized as a graphene thickness measure or efficiency of the exfoliation.

The mechanical exfoliation graphene thin film, will optimally utilize those parameters, and the approaches for the spatial pristine graphene film mapping via the optical microscopy and Raman gave the insights about the concentration of the defects as well as the electrical efficiency. Although there has been an attempt towards using the G & D band peak intensity values, due to the fact that they have a considerably better applicability for the powders, other peak parameters like the 2-D band FWHM may be utilized for the testing of the statistical sizes of the sample. Analyzed parameters have returned from every one of the measurements, based on work-flow that is given in Scheme 1, at first, for the convergence of the data as map have been collected. Such procedure considers whole distribution, and does not make any assumption on the statistical models, and it visualizes the way that the key summary statistics were differed with the addition of more points, beginning from a single data point only.

Figure 1 (a), (b), and (c) exhibit a summary of statistics that change dramatically at first, as the new points have been added prior to becoming smoother; those variations have been divided as well, with 3 areas. Following that point of convergence there will not be much to gain from the collection of additional spectra except increasing the distribution resolution. None-the-less, collecting a smaller number of the data points than that point of convergence may cause erroneous Raman peak parameter distributions. The tolerances to the

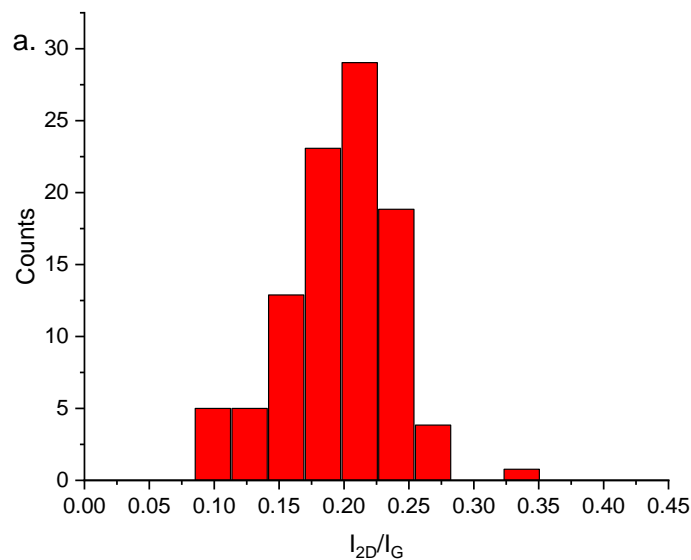
errors in Raman analyses will be dependent upon the analysis aim; in the case where one is simply wishing to search for some considerable alterations to the material after a process or a treatment, a considerably smaller number of the points may be obtained, while a check for the impurities and minority phases in the bulk powder would be requiring a more comprehensive dataset. Flexibility for dealing with any distributions instead of the assumption of a single specified statistical model is significant due to the fact that some of the materials include an arbitrary mix with regular distribution, whereas the others have been dominated by the log-normal distributions, none-the-less other types of the material have uneven distributions that contain 2 phases of the material. In addition to that, two plots of convergence that have been described earlier, an approach which is referred to as the bootstrapping has been utilized for the more sufficient understanding of the under-analyzing effects of the material.

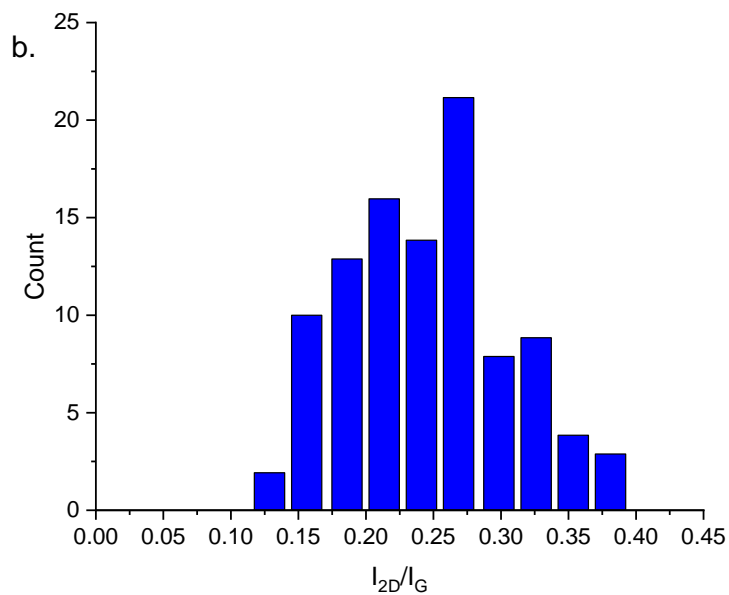




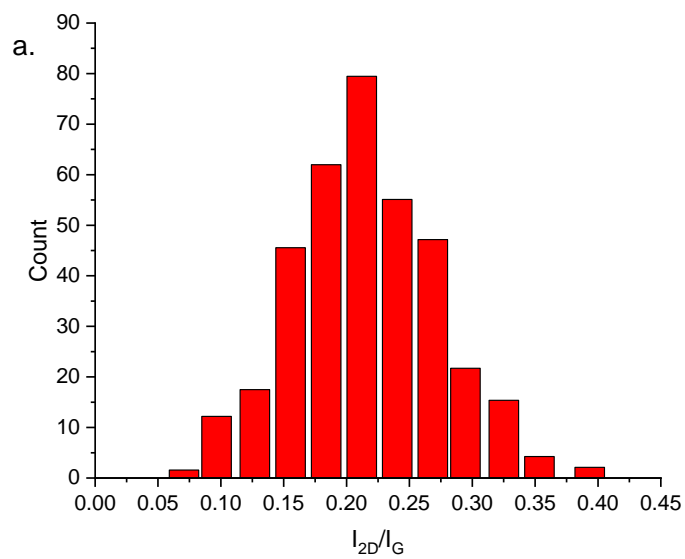
**Figure 1.** The description of summary statistics: a.  $\mu$  refers to the mean, b.  $Q_{25}$ , and  $Q_{75}$  refers to the interquartile range points, and c. the percentiles values.

The bootstrapping carries out repeated analysis of the original dataset's smaller sub-samples gathered and may be utilized for the analysis of scatters in several of those sub-samples about the larger data distribution value. Which uses an approach of the Monte Carlo type for the random selection of the values from a dataset and placing those values in a subsample; which may be analyzed for the purpose of finding the average or even the whole distribution of such sub-sample prior to the repeating of that procedure, for the purpose of generating and analyzing a different arbitrary subsample. Due to the fact that the sub-sample is increased in its size more approximate to the full dataset size, the distribution and the mean are projected to be more approximately resembling the entire distribution of the population as can be seen from Figures 2 and 3.





**Figure 2.** Distribution of the first random value set subsamples and 100 datapoints in these subsamples



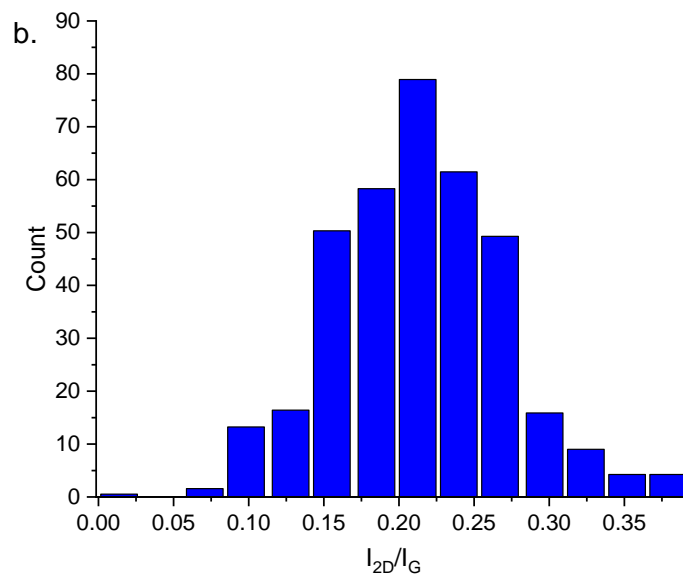


**Figure 3.** Distribution of the first random value set subsamples and 400 datapoints in these subsamples

### Statistical analyses

For attempting any large dataset analyses that contain several of the Raman spectra, it will be significant to be fitting the mathematical models and using parameters in place of every one of the spectra. Each one of which has been fitted in an independent manner from all of the others, which ensures the noisy spectra or the minor components don't have an impact on parameters that have been carried out from another spectrum. Each peak involved in each one of the fits have been validated as well, for the purpose of ensuring the fact that they exist rather than simply the random noise result. The specific needed parameters are dependent upon analysis. However, most often  $I_{2D}/I_G$  and  $I_D/I_G$  were utilized for the characterization of the graphene as well as the associated materials. A 3-D bi-variate histogram heat map has to be emphasized for effective displaying of the entire distributions of every one of those parameters in a simultaneous manner.

In a single graph, allowing easy comparisons against other types of the materials. Through visualizing the trends in the summary statistics and sub-sample distribution evolution, it has been proven possible to be understanding the analyses and making the justifications for using a certain size of the sample. It is obvious that various materials will be requiring bespoke analysis with the thorough justifications; an excessively big number of the data points, in such cases, the Raman spectra, will result in wasting time and increasing the expenses for the companies, however, an excessively small number of the points may be resulting in the mistaken analyses.

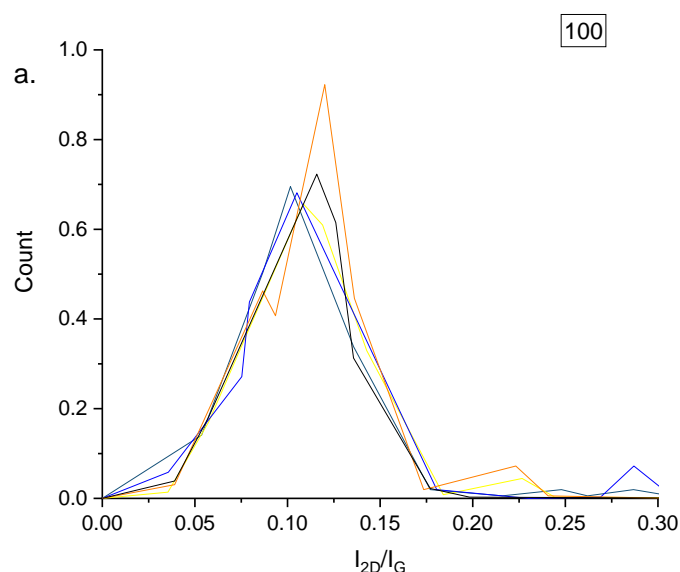
For the purpose of ensuring the fact that 1,024 points are adequate for drawing those conclusions, the 3 independent samples for every one of the materials have been compared. Obviously, there has been noise; none-the-less, every dataset from same material is sufficiently big to be hardly distinguishable from one another, which is why, it has been expected from "true" distribution of this material. Any of the gaps between data and "true" or the distributions of the population may be overlooked. Whereas those datasets have been consistent, the difference between the materials has been noticeable. For the purpose of illustrating that point, 2 commercial GNPs have been contrasted with the use of a statistical approach; the present case study has highlighted the method and the differences in the analyses between the materials. They have been described as a variety of the grades, however, there has not been any information concerning the sizes of the flake, the chemical

functionalization, or the efficiency of the exfoliation that has been provided with those materials and the two have been listed with highly alike Raman spectra.

None-the-less, with the large Raman datasets both those materials have been distinctive. The mono-disperse sample is of considerably sharper distributions in plots of the bootstrap Figure 4 (a), (b), and (c) even in the case of the small size of the sub-sample; those plots have been defined as a way to visualize how differing would an analysis be in the case of the use of smaller sizes of the sample compared to the recorded 1,024. In mono-disperse material cases, if 100 Raman spectra have been only recorded, there would be a degree of the uncertainty as a result of to the shifting in the intensity and the mean between the green lines and the yellow ones. None-the-less, the overall trend has been consistent, and even with 300 of the data points, a variety of the sub-samples are not distinguishable from one another.

Following this point distribution will become more established, even though there remain a few fluctuations with the increase in the size of the sample. As soon as 400 spectra have been included, distribution exhibits a small degree of the change beyond the arbitrary noise and small variations as a result of the potential outliers or slight components that are included already in the analyses. On the other hand, the other commercial sample of the GNP is of a considerably wider  $I_D/I_G$  value ranges, which results in considerable variations even after recording hundreds of the points. Certainly, 500 points are needed prior to the mean, even becoming stable. From that analysis, heterogeneous sample includes 2 elements: a major material fraction that has a low  $I_D/I_G$  and a minor one that has a considerably greater value of  $I_D/I_G$ . The precise amount of the needed measurements would be dependent upon the asked question; none-the-less, those plots exhibit the difficulty to establish the precise distribution even in the case of hundreds of the points.

Such statistically inspired method was as well shown successfully with other materials of the carbon, several of them are of various behaviours and would be requiring various sizes of the sample for their analyses. Here, a multi-step cascade centrifuging process has been purposely avoided for the purification of material and one centrifuging step only has been utilized. With no extensive process of purification, there has been a considerable graphite population that has been discovered in Raman analysis of material. None-the-less, the evidences of the exfoliation via increasing  $I_{2D}/I_G$  have been found





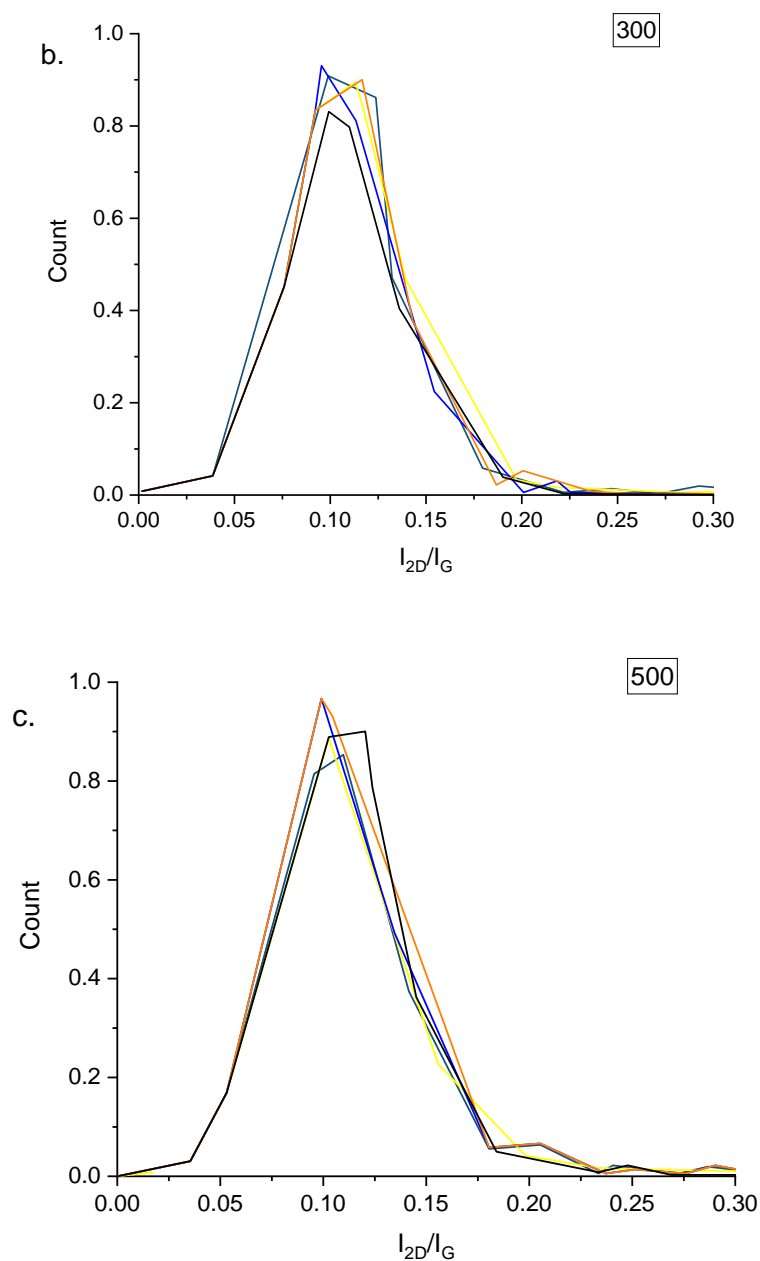


**Figure 4.** The main statistical chart of the products is of high homogeneity: a. 100 points, b. 300 points, and c. 500 points.

Those signals may be hard to be detected from only one Raman spectrum. However, in this paper it has been shown to be possible, and beneficial, for displaying the whole distribution from the nano-material analyses. The size which is required for this type of the distributions for being considered representative may be explained with the described method. The focused has been directed on the detailed GNP discussions in this study, however, the method was applied as well to other materials of the carbon. There is an importance in noting that numbers aren't definitive for the discussed carbon types, due to the fact that the similar materials with various origins can show different behaviors. It's the method and its applications in the determination of the required data points for the convergence are significant. The experimental noise cannot be avoided in the case of collecting the Raman spectra, which is why, for the purpose of understanding the effects of the noise, a model dataset has been produced, on the basis of the actual parameters of the peak to which a regulated degree of the arbitrary noise has been added. Model dataset has

been fitted, then the fitted peak parameters' distribution and convergence from a wide variety of the model spectra, with similar degrees of the noise, have been compared to the increasing levels of the noise. The first one of the observations has been the fact that fitted values were in agreement with the utilized values of the model, in spite of being treated in an independent manner, confirming the program that has been written for fitting Raman datasets is the correct fitting of expected mathematical forms.

### Conclusion

A range of carbonic nanomaterial has been analyzed and a fitting algorithm complemented with a statistical method was applied for peaks parameter extraction. This step facilitates the quantifying of the number of spectra required for material characterization. Also, it will significantly affect graphene measurements through fabrication quality control and product formulating. The signal noises were considered and the uncertainty increased in accordance with a very little impact on the sample sizes.

### References

1. Novoselov, K. S.; Fal'ko, V. I.; Colombo, L.; Gellert, P. R.; Schwab, M. G.; Kim, K. A. Roadmap for Graphene. *Nature* **2012**, *490*, 192–200, DOI: 10.1038/nature11458
2. Ferrari, A. C.; Bonaccorso, F.; Fal'ko, V.; Novoselov, K. S.; Roche, S.; Bøggild, P.; Borini, S.; Koppens, F. H. L.; Palermo, V.; Pugno, N.; Garrido, J. A.; Sordan, R.; Bianco, A.; Ballerini, L.; Prato, M.; Lidorikis, E.; Kivioja, J.; Marinelli, C.; Ryhänen, T.; Morpurgo, A. Science and Technology Roadmap for Graphene, Related Two-Dimensional Crystals, and Hybrid Systems. *Nanoscale* **2015**, *7*, 4598–4810, DOI: 10.1039/C4NR01600A
3. Bianco, A.; Prato, M. Safety Concerns on Graphene and 2D Materials: A Flagship Perspective. *2D Mater.* **2015**, *2*, 030201, DOI: 10.1088/2053-1583/2/3/030201
4. Park, M. V. D. Z.; Bleeker, E. A. J.; Brand, W.; Cassee, F. R.; van Elk, M.; Gosens, I.; de Jong, W. H.; Meesters, J. A. J.; Peijnenburg, W. J. G. M.; Quik, J. T. K.; Vandebriel, R. J.; Sips, A. J. A. M. Considerations for Safe Innovation: The Case of Graphene. *ACS Nano* **2017**, *11*, 9574–9593, DOI: 10.1021/acsnano.7b04120
5. Poland, C. A.; Duffin, R.; Kinloch, I.; Maynard, A.; Wallace, W. A. H.; Seaton, A.; Stone, V.; Brown, S.; MacNee, W.; Donaldson, K. Carbon Nanotubes Introduced into the Abdominal Cavity of Mice Show Asbestos-like Pathogenicity in a Pilot Study. *Nat. Nanotechnol.* **2008**, *3*, 423–428, DOI: 10.1038/nnano.2008.111
6. Kuempel, E. D.; Jaurand, M.-C.; Møller, P.; Morimoto, Y.; Kobayashi, N.; Pinkerton, K. E.; Sargent, L. M.; Vermeulen, R. C. H.; Fubini, B.; Kane, A. B. Evaluating the Mechanistic Evidence and Key Data Gaps in Assessing the Potential Carcinogenicity of Carbon Nanotubes and Nanofibers in Humans. *Crit. Rev. Toxicol.* **2017**, *47*, 1–58, DOI: 10.1080/10408444.2016.1206061
7. Kostarelos, K.; Lacerda, L.; Pastorin, G.; Wu, W.; Wieckowski, S.; Luangsivilay, J.; Godefroy, S.; Pantarotto, D.; Briand, J.-P.; Muller, S.; Prato, M.; Bianco, A. Cellular Uptake of Functionalized Carbon Nanotubes Is Independent of Functional Group and Cell Type. *Nat. Nanotechnol.* **2007**, *2*, 108–113, DOI: 10.1038/nnano.2006.209
8. Schipper, M. L.; Nakayama-Ratchford, N.; Davis, C. R.; Kam, N. W. S.; Chu, P.; Liu, Z.; Sun, X.; Dai, H.; Gambhir, S. S. A Pilot Toxicology Study of Single-Walled Carbon Nanotubes in a Small Sample of Mice. *Nat. Nanotechnol.* **2008**, *3*, 216–221, DOI: 10.1038/nnano.2008.68
9. Kagan, V. E.; Konduru, N. V.; Feng, W.; Allen, B. L.; Conroy, J.; Volkov, Y.; Vlasova, I. I.; Belikova, N. A.; Yanamala, N.; Kapralov, A.; Tyurina, Y. Y.; Shi, J.; Kisin, E. R.; Murray, A. R.; Franks, J.; Stolz, D.; Gou, P.; Klein-Seetharaman, J.; Fadeel, B.; Star, A. Carbon Nanotubes Degraded by Neutrophil Myeloperoxidase Induce Less Pulmonary Inflammation. *Nat. Nanotechnol.* **2010**, *5*, 354–359, DOI: 10.1038/nnano.2010.44
10. Bhattacharya, K.; Mukherjee, S. P.; Gallud, A.; Burkert, S. C.; Bistarelli, S.; Bellucci, S.; Bottini, M.; Star, A.; Fadeel, B. Biological Interactions of Carbon-Based Nanomaterials:

- From Coronation to Degradation. *Nanomedicine* **2016**, *12*, 333–351, DOI: 10.1016/j.nano.2015.11.011
11. Raccichini, R.; Varzi, A.; Passerini, S.; Scrosati, B. The Role of Graphene for Electrochemical Energy Storage. *Nat. Mater.* **2015**, *14*, 271–279, DOI: 10.1038/nmat4170
  12. Moon, I. K.; Lee, J.; Ruoff, R. S.; Lee, H. Reduced Graphene Oxide by Chemical Graphitization. *Nat. Commun.* **2010**, *1*, 73, DOI: 10.1038/ncomms1067
  13. Stoller, M. D.; Park, S.; Zhu, Y.; An, J.; Ruoff, R. S. Graphene-Based Ultracapacitors. *Nano Lett.* **2008**, *8*, 3498–3502, DOI: 10.1021/nl802558y
  14. Li, C.; Shi, G. Functional Gels Based on Chemically Modified Graphenes. *Adv. Mater.* **2014**, *26*, 3992–4012, DOI: 10.1002/adma.201306104
  15. Herrera-Alonso, M.; Abdala, A. A.; McAllister, M. J.; Aksay, I. A.; Prud'homme, R. K. Intercalation and Stitching of Graphite Oxide with Diaminoalkanes. *Langmuir* **2007**, *23*, 10644–10649, DOI: 10.1021/la0633839
  16. Hung, W. S.; Tsou, C. H.; De Guzman, M.; An, Q. F.; Liu, Y. L.; Zhang, Y. M.; Hu, C. C.; Lee, K. R.; Lai, J. Y. Cross-Linking with Diamine Monomers to Prepare Composite Graphene Oxide-Framework Membranes with Varying d-Spacing. *Chem. Mater.* **2014**, *26*, 2983–2990, DOI: 10.1021/cm5007873
  17. Banda, H.; Daffos, B.; Périé, S.; Chenavier, Y.; Dubois, L.; Aradilla, D.; Pouget, S.; Simon, P.; Crosnier, O.; Taberna, P. L.; Duclairoir, F. Ion Sieving Effects in Chemically Tuned Pillared Graphene Materials for Electrochemical Capacitors. *Chem. Mater.* **2018**, *30*, 3040–3047, DOI:10.1021/acs.chemmater.8b00759
  18. Bourlinos, A. B.; Gournis, D.; Petridis, D.; Szabó, T.; Szeri, A.; Dékány, I. Graphite Oxide: Chemical Reduction to Graphite and Surface Modification with Primary Aliphatic Amines and Amino Acids. *Langmuir* **2003**, *19*, 6050–6055, DOI: 10.1021/la026525h
  19. Merlet, C.; Péan, C.; Rotenberg, B.; Madden, P. A.; Daffos, B.; Taberna, P. L.; Simon, P.; Salanne, M. Highly Confined Ions Store Charge More Efficiently in Supercapacitors. *Nat. Commun.* **2013**, *4*, 2701, DOI: 10.1038/ncomms3701